Published in final edited form as:

Int J Cancer. 2017 November 15; 141(10): 2131–2142. doi:10.1002/ijc.30904.

GPR55 receptor antagonist decreases glycolytic activity in PANC-1 pancreatic cancer cell line and tumor xenografts

Michel Bernier[1], **Jonathan Catazaro**[#2], **Nagendra S. Singh**[#3], **Artur Wnorowski**[4], **Anna Boguszewska-Czubara**[5], **Krzysztof Jozwiak**[4], **Robert Powers**[2], and **Irving W. Wainer**[3,6,#]

[1]Translational Gerontology Branch, Intramural Research Program of the National Institute on Aging, National Institutes of Health, Baltimore, MD 21224, USA [2]Department of Chemistry, University of Nebraska-Lincoln, Lincoln, NE 68588-0304, USA [3]Laboratory of Clinical Investigation, Intramural Research Program of the National Institute on Aging, National Institutes of Health, Baltimore, MD 21224, USA [4]Department of Biopharmacy, Medical University of Lublin, 20-093 Lublin, Poland [5]Department of Medical Chemistry, Medical University of Lublin, 20-093 Lublin, Poland [6]Mitchell Woods Pharmaceuticals, Shelton, CT 06484, USA

[#] These authors contributed equally to this work.

Abstract

The Warburg effect is a predominant metabolic pathway in cancer cells characterized by enhanced glucose uptake and its conversion to L-lactate and is associated with upregulated expression of HIF-1α and activation of the EGFR-MEK-ERK, Wnt-β-catenin and PI3K-AKT signaling pathways. (*R,R'*)-4'-methoxy-1-naphthylfenoterol ((*R,R'*)-MNF) significantly reduces proliferation, survival, and motility of PANC-1 pancreatic cancer cells through inhibition of the GPR55 receptor. We examined (*R,R'*)-MNF's effect on glycolysis in PANC-1 cells and tumors. Global NMR metabolomics was used to elucidate differences in the metabolome between untreated and (*R,R'*)-MNF-treated cells. LC/MS analysis was used to quantify intracellular concentrations of β-hydroxybutyrate, carnitine and L-lactate. Changes in target protein expression were determined by Western blot analysis. Data was also obtained from mouse PANC-1 tumor

[#]**Correspondence should be sent to:** Irving W. Wainer, Mitchell Woods Pharmaceuticals, Four Corporate Drive, Suite 287, Shelton, CT 06484, USA. Tel.: + 1 202 255 7039, iwwainer@mitchellwoods.com or iwainer@hotmail.com.

Conflict of interest: Drs. Bernier and Wainer are listed as co-inventors on an issued patent for (*R,R'*)-MNF and other fenoterol derivatives and in submitted patents for their use in glioblastoma and astrocytoma tumors. Drs. Bernier and Wainer have assigned their rights in the patents to the U.S. government, but will receive a percentage of any royalties that may be received by the government. Dr. Wainer is currently Chief Scientific Officer of Mitchell Woods Pharmaceuticals, which has an exclusive license for the use of (*R,R'*)-MNF and related compounds in the treatment of pancreatic, liver and brain cancers. The remaining authors state no conflict of interest.

Authorship Contributions

Participated in research design: Bernier, Jozwiak, Powers, Wainer
Conducted experiments and data acquisition: Singh, Catazaro, Wnorowski, Boguszewska-Czubara
Performed data analysis and interpretation: Singh, Catazaro, Wnorowski, Bernier, Powers, Wainer
Wrote or contributed to the writing of the manuscript: Bernier, Powers, Wainer
Study supervision: Bernier, Jozwiak, Powers, Wainer

Novelty and Impact of the work: Glycolysis is an interrelated multi-component system and a key target in cancer therapy. Here we investigate the effect of the GPR55 inhibitor (*R,R'*)-4-methoxynaphthylfenoterol on glycolysis in human PANC-1 pancreatic cancer cells and murine xenograft model using global NMR metabolomics, LC/MS analysis, and immunoblotting techniques. The data indicate that (*R,R'*)-4-methoxy-1-naphthylfenoterol reduces glycolysis in PANC-1 cells through a multifaceted effect based upon reduced expression and function at multiple controlling sites in the glycolytic pathway.

xenografts after administration of (*R,R'*)-MNF. Metabolomics data indicate that (*R,R'*)-MNF altered fatty acid metabolism, energy metabolism, and amino acid metabolism and increased intracellular concentrations of β-hydroxybutyrate and carnitine while reducing L-lactate content. The cellular content of phosphoinositide-dependent kinase-1 and hexokinase 2 was reduced consistent with diminished PI3K-AKT signaling and glucose metabolism. The presence of the GLUT8 transporter was established and found to be attenuated by (*R,R'*)-MNF. Mice treated with (*R,R'*)-MNF had significant accumulation of L-lactate in tumor tissue relative to vehicle-treated mice, together with reduced levels of the selective L-lactate transporter MCT4. Lower intratumoral levels of EGFR, pyruvate kinase M2, β-catenin, hexokinase 2 and P-glycoprotein were also observed. The data suggest that (*R,R'*)-MNF reduces glycolysis in PANC-1 cells and tumors through reduced expression and function at multiple controlling sites in the glycolytic pathway.

Keywords

Pancreatic cancer; Warburg effect; metabolic reprogramming; PKM2; metabolomics; L-lactate

Introduction

Aerobic glycolysis, the "Warburg effect", is a predominant metabolic pathway in cancer cells characterized by enhanced glucose uptake and its conversion to L-lactate.[1,2] This pathway is a multi-component system and includes glucose transporter (GLUT)-facilitated cellular uptake of glucose, conversion of glucose to glucose-6-phosphate via hexokinase (HK), formation of pyruvate from phosphoenolpyruvate catalyzed by pyruvate kinase M2 (PKM2), conversion of pyruvate to L-lactate by lactate dehydrogenase A (LDHA), and the export of L-lactate by the MCT4 isoform of the monocarboxylate transporter family.[3] Some of the metabolic intermediates of glycolysis include those implicated in the pentose phosphate pathway and processes leading to the biosynthesis of hexosamine, glycerol-3-phosphate and serine/glycine.[3]

Recent studies of metabolic reprogramming indicate that the "Warburg effect" is only one aspect of several interrelated processes associated with tumorigenesis.[3,4] This integrated system includes interaction between tumors and their microenvironments via transporter and symporter proteins such as MCT1 and MCT4, the Na^+–HCO_3^- cotransporter NBCn1, carbonic anhydrases, and the Na^+/H^+ exchanger. Metabolic reprogramming is also associated with increased expression and stabilization of hypoxia-inducible factors (HIF), primarily HIF-1α, and enhanced intracellular signaling through the EGFR-MEK-ERK, Wnt-β-catenin and PI3K-3-phosphoinositide-dependent protein kinase-1 (PDK1)-AKT pathways.[2,5]

Because metabolic reprogramming is a central component of tumor growth, metastasis, and immunoresistance, blunting its effects is a key therapeutic objective.[4,5] One approach is targeting specific facets of the glycolytic process using inhibitors such as 2-deoxyglucose, lonidamine, and 3-bromopyruvate.[2,6] The combination of glycolytic inhibitors with other treatment modalities has increased the effectiveness of cisplatin in ovarian cancer cells[6] and photodynamic therapy in breast cancer cells.[7] However, the interrelationships and

redundancies involved in metabolic reprogramming require the targeting of multiple aspects of the glycolytic process, exemplified by the use of 2-deoxyglucose and the mitochondrial respiration inhibitor metformin.[8]

(*R,R'*)-4'-Methoxy-1-naphthylfenoterol ((*R,R'*)-MNF) is a bi-functional anticancer agent that inhibits the G protein-coupled receptor GPR55 and activates the β_2-adrenergic receptor (β_2-AR)[9]. GPR55 is a cannabinoid receptor-like G protein-coupled receptor that has pro-oncogenic properties and whose expression correlates with tumor aggressiveness in a number of tumors including pancreatic, breast and glioblastoma.[10–12] We have recently demonstrated that in human-derived PANC-1 pancreatic cancer cells (*R,R'*)-MNF-mediated GPR55 inhibition results in an attenuation of intracellular signaling through the EGFR-MEK-ERK, Wnt-β-catenin and PI3K-AKT pathways, lower nuclear concentrations of HIF-1α and the phospho-active forms of PKM2 (pSer37-PKM2) and β-catenin (pTyr333-β-catenin), and reduced expression of β-catenin, PKM2, HIF-1α, EGFR and transporters associated with multidrug resistance.[13] Similar effects were observed with the human-derived breast cancer MDA-MB-231 and glioblastoma U87MG cell lines.[13] The data suggest that (*R,R'*)-MNF may be useful in the alleviation of metabolic reprogramming through attenuation of the expression and function of proteins involved in the glycolytic process. In the current study, we incubated PANC-1 cells with (*R,R'*)-MNF and identified resulting changes in metabolic patterns and protein expression using non-targeted and targeted metabolomics and Western blot analysis. In addition, changes in select target proteins and metabolites were determined in plasma and tumor tissue samples obtained from (*R,R'*)-MNF-treated and control mice bearing PANC-1-derived tumor xenografts.

Materials and Methods

Materials.

(*R,R'*)-MNF was synthesized as previously described.[14] Lactate (purity ≥ 98%), 3-hydroxybutyrate (purity ≥ 98%), carnitine (purity ≥ 98%), *p*-aminohippuric acid (purity ≥ 98%), human recombinant insulin (dry powder), methanol (HPLC grade), acetonitrile (HPLC grade) and formic acid were obtained from Sigma-Aldrich (St. Louis, MO, USA). Dulbecco's modified Eagle's medium (DMEM), RPMI-1640 medium, Eagle's Minimum Essential Medium (EMEM), trypsin solution, phosphate-buffered saline (PBS), fetal bovine serum (FBS), 100X solutions of sodium pyruvate (100 mM), L-glutamine (200 mM), and penicillin/streptomycin (a mixture of 10,000 units/mL) were obtained from Quality Biological (Gaithersburg, MD, USA).

Cell Culture.

PANC-1 pancreatic tumor, MDA-MB-231 and MCF-7 breast cancer, and rat-derived C6 glioblastoma cell lines were purchased from ATCC (Manassas, VA, USA). Upon receipt, cells were expanded for a few passages to enable the generation of new frozen stocks. Cells were resuscitated as needed and used for fewer than 6 months after resuscitation (no more than 10 passages). ATCC performs thorough cell line authentication utilizing Short Tandem Repeat (STR) profiling.

PANC-1 and C6 cells were maintained in DMEM with L-glutamine supplemented with 10% FBS and 1% penicillin/streptomycin. MDA-MB-231 cells were maintained in RPMI-1640 supplemented with 10% FBS and 1% penicillin/streptomycin and MCF-7 cells were maintained in EMEM with L-glutamine supplemented with 10% FBS and 0.01 $mg \cdot ml^{-1}$ human recombinant insulin. Cells were maintained in a controlled environment (37°C under humidified 5% CO_2 in air), and the medium was replaced every 2–3 days. Prior to experiments, cells were seeded on 100 × 20 mm tissue culture plates and grown to ~70% confluency unless stated otherwise.

Cell Treatment.

In the first series of experiments, the original media was replaced with media containing vehicle (0.01% DMSO) or (*R,R'*)-MNF (0.01, 0.10, 0.50 and 1.00 μM) for 24h. The medium was removed, and cells were collected and processed for immunoblot analysis. In a second series of experiments, PANC-1 cells were treated with vehicle (0.01% DMSO) or (*R,R'*)-MNF (0.50 and 1.00 μM) for 24h after which cells were washed, and then collected and processed for NMR or LC/MS analysis. In the last series of experiments, MDA-MB-231 and MCF-7 cells were treated with vehicle (0.01% DMSO) or (*R,R'*)-MNF (1.00 μM) for 24h and processed for LC/MS analysis. All experiments were repeated three times on three separate days, unless stated otherwise.

Glucose consumption and lactate production in C6 cells.

To assess glucose consumption and lactate production, C6 cells were seeded in 48-well plates at 18×10^3 cells/well and after 24h, the culture medium was removed and replaced with serum-free medium containing (*R,R'*)-MNF (0.02 or 0.20 μM) or vehicle (DMSO, 0.1%) for 48 h. Glucose and L-lactate concentrations in the incubation media were periodically monitored using the Liquick Cor-Glucose and Liquick Cor-Lactate Diagnostic Kits (Cormay, Lublin, Poland). Measurements were carried out according to the manufacturer's protocols. In a separate series of experiments, C6 cells were pre-treated for 30 min with the highly selective β2-AR inhibitor ICI-118,551 (0.10 μM) in serum-free media and then incubated with (*R,R'*)-MNF (0.02 or 0.20 μM) for 48h. In addition, cells were pretreated for 30 min with (*R,R'*)-MNF in serum-free media and then stimulated with the GPR55 agonist O-1620 (5.00 μM) for 48 h. Both the glucose and lactate concentrations in the incubation media were determined.

PANC-1 Tumor Xenograft in Mice.

Female Balb/c nude mice (aged between 6–8 weeks, weight 18–20 g) were purchased from HFK Bioscience Co., Ltd. (Beijing, China) and maintained under pathogen-free conditions with a 12-h light/12-h dark cycle. Animals had free access to drinking water and were fed *ad libitum* with normal chow. Each mouse was inoculated subcutaneously at the right flank region with PANC-1 cells (5×10^6) in 0.1mL of PBS for tumor development. All animals were weighed and the tumor volumes measured in two dimensions using a caliper, and the volume expressed in mm^3 using the formula: $V = 0.5\ a \times b^2$, where a and b are the long and short diameters of the tumor, respectively. The treatments were started at day 8 when the mean tumor size reached 164 mm^3, at which time the mice were assigned into two groups (n = 10) using randomized block design based on their tumor volumes. Mice received an i.p.

injection of either vehicle (20% hydroxypropyl-β-cyclodextrin) or 10 mg/kg (*R,R'*)-MNF once daily for 16 days adjusted to 25 mg/kg for the last 5 days. The dosing volume was adjusted according to weight (10 μL/g). At the end of the study, plasma samples were obtained and the animals were euthanized by cervical extension and the tumors collected, weighed, divided into three portions and snap frozen. All protocols were approved by the Animal Care and Use Committee at CrownBio (AN-1407–009-164), which are based on "the Guide for the Care and Use of Laboratory Animals" (NRC 2011).

Western Blot Analysis.

Cells and frozen tumor tissues were lysed in radioimmunoprecipitation buffer containing EGTA and EDTA (Boston BioProducts, Ashland, MA, USA) supplemented with protease inhibitor cocktail (Sigma-Aldrich) and phosphatase inhibitor cocktail sets I and II (Calbiochem, San Diego, CA, USA). Protein concentration in clarified lysates was determined using the bicinchoninic acid reagent (Thermo Fisher Scientific, Waltham, MA, USA). Proteins (20 μg/well) were separated on 4–12% precast gels (Invitrogen, Carlsbad, CA, USA) using SDS-polyacrylamide gel electrophoresis under reducing conditions and then electrophoretically transferred onto polyvinylidene fluoride membrane (Invitrogen). Western blots were performed according to standard methods, which involved a blocking step in Tris-buffered saline/0.1% Tween-20 (TBS-T) supplemented with 5% non-fat milk and incubation with primary antibodies of interest. All antibodies were detected with horseradish peroxidase-conjugated secondary antibodies (Santa Cruz Biotechnology, Dallas, TX, USA) and visualized by enhanced chemiluminescence (ECL Plus, GE Healthcare, Piscataway, NJ, USA). Quantification of the protein bands was performed by volume densitometry using ImageJ software (National Institutes of Health, Bethesda, MD, USA) and followed by normalization to β-actin. The primary antibodies used in this study were raised against EGFR (sc-03), MCT4 (sc-50329), GLUT8 (sc-30108), and β-catenin (sc-7199) (Santa Cruz Biotechnology); PKM2 (ab38237) and β-actin (ab6276) (Abcam, Cambridge, MA, USA); HK2 (cat. #2867) and PDK1 (cat. #3062S) (Cell Signaling Technology, Beverly, MA, USA). The antibodies were used at the dilution recommended by the manufacturers.

NMR Data Collection and Analysis.

One-dimensional (1D) ^{1}H NMR data collection and analysis were performed as described previously.[15,16] Briefly, six biological replicates per class were prepared for NMR analysis by dissolving lyophilized cell extracts in 600 μL of 50 mM phosphate buffer (pH 7.2, uncorrected) in 99.8% D_2O (Cambridge Isotope Laboratories, Tewksbury, MA, USA) with 50 μM of 3-(tetramethysilane)propionic acid-2,2,3,3-d_4 (TMSP). NMR spectra were recorded at 298K on a Bruker Avance III-HD 700 MHz spectrometer equipped with a 5 mm inverse quadruple-resonance (^{1}H, ^{13}C, ^{15}N, ^{31}P) cryoprobe with cooled ^{1}H and ^{13}C channels and a *z*-axis gradient. A SampleJet automated sample changer with Bruker ICON-NMR software was used to automate the NMR data collection. 1D ^{1}H spectra were collected using excitation sculpting to remove the solvent signal and avoid any need for baseline corrections.[17] A total of 16k data points with a spectral width of 5482.5 Hz, 8 dummy scans, and 256 scans were used to obtain each spectrum.

The 1D ^{1}H NMR spectra were processed and analyzed using our MVAPACK metabolomics toolkit (http://bionmr.unl.edu/mvapack.php).[18] The 1D ^{1}H NMR spectra were Fourier-transformed and phased prior to normalization using phase scatter correction.[19] Residual solvent peaks and noise regions were removed and the spectra were referenced to TMSP at 0.0 ppm. The spectra were then binned using an intelligent adaptive binning algorithm[20] or aligned with the Icoshift algorithm.[21] Data was scaled using the Pareto method prior to principal component analysis (PCA) or orthogonal projections to latent structures (OPLS) analysis. Binned data was used for the PCA model, whereas full spectral data was utilized for the OPLS models.

The validated OPLS models enabled the generation of back-scaled loadings plots to identify spectral features (NMR peaks) that primarily contribute to the observed group separation. The relative peak intensities in these “pseudospectra” highlight the magnitude of the metabolite’s contribution to the group separation in the OPLS scores plot. Similarly, the relative sign of the peak indicates if the metabolite’s concentration increases (negative) or decreases (positive) due to (*R,R’*)-MNF treatment. All non-overlapping ^{1}H NMR peaks identified by the back-scaled loading plots as a major contributor to group separation in the OPLS scores plot were assigned to a metabolite using the Chenomx NMR suite 7.0 (Chenomx Inc., Edmonton, Alberta, Canada). ^{1}H NMR peaks with significant overlap and multiple metabolite assignments were excluded from further analyses.

Identified metabolites in the 1D ^{1}H NMR spectra were submitted to the Human Metabolome Database (HMDB) for HMDB ID retrieval. The IDs of the metabolites were subsequently entered into the MetPA webserver for metabolic pathway analysis (http://metpa.metabolomics.ca/MetPA/faces/Home.jsp).[22] The *Homo sapiens* pathway library was selected for analysis and all compounds in the pathways were used.

Statistical Analysis.

OPLS model results were validated using CV-ANOVA significance testing.[23] Fractions of explained variation (R^2_X and R^2_Y) were computed during the OPLS model training. The OPLS models were also internally cross-validated using seven-fold Monte Carlo cross-validation to compute Q^2 values.[24,25] The R^2 (degree of fit) and Q^2 (predictive ability) metrics were also calculated for the PCA model. Ellipses in the PCA and OPLS scores plot were generated with our PCA/PLS-DA utilities[26] implemented in MVAPACK;[18] and correspond to the 95% confidence limits from a normal distribution for each group.

Statistical comparisons between treated and control groups were performed using paired Student’s t-tests. For the *set* of metabolites identified to be statistically different between untreated and (R,R’)-MNF-treated PANC-1 cells based on the Student’s t-test *p*-values, the Benjamini-Hochberg method was then applied to the t-test *p*-values to control for false positives[27] in the multiple comparisons. Data are expressed as relative fold change ± standard deviation. *P* values ≤ 0.05 were considered significant.

Results

Global cellular metabolomics in PANC-1 cells.

A global NMR metabolomics study was undertaken to elucidate differences in the metabolome between untreated and (*R,R'*)-MNF-treated PANC-1 cells. Two-dimensional (2D) PCA scores plot was generated from the data and a statistically significant separation ($p \leq 2.5\times10^{-6}$) between the untreated (open circles) and the (*R,R'*)-MNF-treated groups (gray and filled circles) is clearly apparent in the PCA scores plot (Figure 1A). There is no overlap in the ellipses, which corresponds to the 95% confidence intervals for a normal distribution, for each group and the relative PCA separation between the untreated and (*R,R'*)-MNF-treated groups is dose-dependent (Figure 1A). The PCA model yielded R^2 and Q^2 values of 0.7598 and 0.5381, respectively, which are consistent with a reliable model.[28] The results indicate that treatment of PANC-1 cells with (*R,R'*)-MNF produces a statistically significant and dose-dependent change in the cellular metabolome.

Two OPLS models were also generated from the NMR dataset to identify the metabolites primarily contributing to the group separation in the PCA scores plot. The OPLS models were generated from a comparison between the untreated PANC-1 cells with either the 0.5 μM (*R,R'*)-MNF or 1 μM (*R,R'*)-MNF treatment (Supplemental Information Figure S1A, Figure S1C). Both OPLS models indicated a clear separation between treated and untreated PANC-1 cells. The quality of the OPLS-DA models was evaluated on the basis of cross-validation by a Monte Carlo leave-n-out procedure[24,25] and CV-ANOVA.[23] The OPLS model based on the 0.5 μM (*R,R'*)-MNF treatment yielded an R^2 of 0.9976, a Q^2 of 0.9357 and CV-ANOVA (p=0.03). Similarly, the OPLS model based on the 1 μM MNF treatment yielded an R^2 of 0.9949, a Q^2 of 0.9182 and CV-ANOVA (p=0.05). These results indicate that the two OPLS models are valid. Importantly, a comparison only between the two (*R,R'*)-MNF treatment groups indicates a complete lack of statistical significance. A separation was not observed in a PCA scores plot and the CV-ANOVA p-value for an OPLS model was above 0.05 (data not shown). This indicates that the same set of metabolites was affected regardless of the (*R,R'*)-MNF dose.

Back-scaled loading plots (Supplementary Information Figures S1B and S1D) generated from the OPLS-DA model were used to identify the 1D ^{1}H NMR peaks that contribute to the class separation in the scores plot (see Materials & Methods section for details) and relative metabolite concentration changes were plotted (Figure 1B). Statistically significant concentration changes were identified for branched chain amino acids (BCAAs), β-hydroxybutyrate, L-lactate, alanine, leucine, lysine, creatine, carnitine, and glycerol/glycine. The identified metabolites were subjected to metabolic pathway analysis using the MetPA webserver.[22] MetPA uses pathway enrichment to identify relevant metabolic pathways that may be perturbed in the study. A total of 27 pathways were identified with 8 reaching significance ($p<0.05$) (Figure 1C). In each of the significant pathways, 2 or more metabolite "hits" were found in the input metabolite list. The relevant identified pathways are, therefore, dependent on the input list and may not completely cover all of the perturbed pathways in the metabolome of the (*R,R'*)-MNF-treated and untreated PANC-1 cells. Aminoacyl-tRNA biosynthesis, valine, leucine, and isoleucine biosynthesis/degradation,

glycine, serine, and threonine metabolism, propanoate metabolism, alterations in the glycerophospholipid metabolism and lysine degradation were found to be relevant in PANC-1 cells after treatment with (*R,R'*)-MNF (Figure 1C).

Targeted metabolomics.

In the next series of experiments, we developed a LC-MS method to quantify intracellular concentrations of carnitine, L-lactate and β-hydroxybutyrate (Supplementary Information, LC/MS Analysis, Figures S1E, S1G), as the results from the global NMR metabolomics study had identified these compounds as being significantly affected by (*R,R'*)-MNF. (*R,R'*)-MNF treatment produced significant increases in the intracellular concentration of carnitine (127 ± 3%) and β-hydroxybutyrate (125 ± 4%), while significantly reducing L-lactate level (50 ± 9%) relative to Control (Figure 1D). Similar results were obtained after (*R,R'*)-MNF treatment of MCF-7 and MDA-MB-321 breast cancer cells (Figure 1E).

Immunoblot analysis of PANC-1 cells.

The data from the metabolomics studies indicate that (*R,R'*)-MNF affects metabolic reprogramming in PANC-1 cells. The ability of (*R,R'*)-MNF to reduce PKM2 protein levels in these cells[13] led us to investigate its impact on the expression of two other key proteins involved in the glycolytic pathway, GLUT8 and HK2 (Figure 2A). Treatment of PANC-1 cells with (*R,R'*)-MNF for 24 h led to a dose-dependent reduction in the cellular content of both proteins (Figure 2B). Moreover, the significant reduction in PDK1 protein levels in (*R,R'*)-MNF-treated PANC-1 cells (Figure 3B) likely contributed to the diminished accumulation of phospho-active forms of AKT (p-Ser473) and β-catenin (p-Tyr333) that was previously reported.[13] Representative full-length immunoblots for GLUT8, HK2, and PDK1 are presented in Supplemental Information (Figure S2A). Previous studies of (R,R')-MNF in PANC-1 cells demonstrated a significant reduction in the levels of p-glycoprotein (PGP) and breast cancer resistance protein (BCRP) with a concomitant increase in sensitivity to doxorubicin and gemcitabine cytotoxicity.[13] In this study, tumor tissues obtained from (R,R')-MNF-treated mice displayed a significantly lower accumulation of PGP and reduced BCRP levels (Figure S2B, S2C).

Impact of (R,R')-MNF on PANC-1 tumor xenografts in nude mice.

In the PANC-1 xenograft study, the initial (*R,R'*)-MNF dose of 10 mg/kg was escalated to 25 mg/kg on Day 16 of a 21-day study. The dosing regimen did not affect tumor growth as determined by the tumor volumes at termination: 735 ± 69 mm^3 versus 802 ± 39 mm^3 for Control and (*R,R'*)-MNF-treated groups, respectively. As part of the study protocol, tumor tissues and plasma samples were collected and analyzed for L-lactate and ketone bodies. At the conclusion of the study, the plasma concentration of L-lactate in the (*R,R'*)-MNF-treated mice was significantly lower compared with vehicle-treated animals, 3.25 ± 0.83 mM and 5.56 ± 0.83 mM, respectively ($p<0.001$) while the L-lactate levels were increased in tumor tissues obtained from the (*R,R'*)-MNF-treated cohort relative to Control, 39.1 ± 3.2 mM and 30.7 ± 3.1 mM respectively ($p<0.001$) (Figure 2C). Treatment with (*R,R'*)-MNF resulted in a significant increase in the concentration of ketone bodies in the plasma, 0.59 ± 0.08 mM and 0.33 ± 0.11 mM, for (*R,R'*)-MNF-treated and Control mice, respectively ($p<0.001$), and tumor tissues, 1.02 ± 0.13 mM and 0.56 ± 0.18 mM, respectively ($p<0.001$) (Figure 2D).

Immunoblot analysis performed on tumor protein extracts indicated a significant downregulation in the total levels of EGFR, PKM2, β-catenin, MCT4, and HK2 (Figures 2E–2H), as well as PgP but not BCRP (Supplemental Information Figures S2B and S2C).

Glucose uptake studies in C6 cells.

The anticancer effect of (*R,R'*)-MNF observed in studies with rat C6 glioma cells and xenograft C6 tumor models[9,29] suggests that (*R,R'*)-MNF treatment may also affect glycolysis in these tumors. Therefore, glucose uptake and L-lactate export were assessed in the spent medium of C6 cells over a 48-h incubation period with (*R,R'*)-MNF. Treatment of C6 cells with (*R,R'*)-MNF (0.02 and 0.2 μM) maintained the amount of glucose in the media relative to control (Figure 3A) while significantly decreasing the L-lactate concentration (Figure 3B, $p<0.001$ for both metabolites). No significant differences were observed between the effects produced by the two (*R,R'*)-MNF concentrations.

Because (*R,R'*)-MNF is a potent β_2-AR agonist[9], we investigated whether pretreatment with the β_2-AR inhibitor ICI-118,551 blunts (*R,R'*)-MNF responsiveness in C6 cells. The results indicated that ICI-118,551 had no inhibitory effect (Figure 3C). In contrast, stimulation of C6 cells with the GPR55 agonist O-1602 elicited significant increases in glucose consumption (less glucose remained in the culture media) and lactate secretion, which were blocked by pretreatment with (*R,R'*)-MNF (Figure 3D).

Discussion

In our previous study, we demonstrated that the incubation of PANC-1 cells with (*R,R'*)-MNF significantly attenuates PI3K-AKT and EGFR-MEK-ERK signaling, reducing nuclear translocation of HIF-1α and pTyr333-β-catenin, with subsequent decreases in the expression of EGFR, HIF-1α, β-catenin, and multidrug resistance proteins.[13] We also demonstrated that the incubation of PANC-1 cells with GPR55 inhibitors reduces the cellular levels of PKM2 and the nuclear translocation of pSer37-PKM2.[13] PKM2 catalyzes the conversion of phosphoenolpyruvate into pyruvate and is one of the rate limiting enzymes in glucose metabolism.[5] It also plays a key role in metabolic reprogramming, as ERK-dependent phosphorylation of PKM2 and nuclear translocation of pSer37-PKM2 have been shown to promote the Warburg effect and is associated with increased glycolytic flux, oncogene transactivation, epigenetic changes, and expression of proteins associated with the glycolytic pathway.[30–32] It is interesting to note that in the PANC-1 tumor tissues obtained from animals treated with (R,R')-MNF, there was clear reduction in the levels of the PKM2, EGFR, and β-catenin proteins relative to control-treated animals (Figure 2G) as was the content in PGP (Figure S2C). This suggests that in the tumor tissues, treatment with (R,R')-MNF reduces nuclear pSer37-PKM2 levels and that this effect plays a role in the attenuation of glycolytic flux.

In the current study, we expanded the investigation into the effect of (*R,R'*)-MNF on the expression of proteins associated with glycolysis (Figure 4A). We first determined that there was a dose-dependent decrease in the expression of PDK1, a key component of the PI3K-AKT pathway[33], which is compatible with the previously observed reduction in the levels of pSer473-AKT, the phospho-active form of AKT.[13] Secondly, we determined that (*R,R'*)-

MNF attenuated HK2 protein levels, which is consistent with the link between the PI3K-AKT-PKM2 activation and HK2 expression.[34–36] HK2 plays a key role in glycolysis,[34] and elevated expression of HK2 and PKM2 are associated with an unfavorable clinical outcome and upregulated lactate production in pancreatic tumors.[37]

We next employed a metabolomics approach to determine if the reduction in the expression and activation of PKM2 and HK2 affected glycolysis in PANC-1 cells (Figure 4B). Untargeted metabolomics is an approach designed to identify disease-specific metabolic profiles and treatment-induced changes in these profiles, and to explore biochemical networks.[38] This approach has previously been employed to study drug-induced effects in pancreatic tumor models.[39,40] In the current study, incubation of PANC-1 cells with (*R,R'*)-MNF led to the up-regulation of BCAAs, β-hydroxybutyrate, alanine, leucine, lysine, creatine, carnitine, and glycerol/glycine, while causing a significant reduction in L-lactate. Incubation with (*R,R'*)-MNF produced similar effects on the intracellular concentrations of β-hydroxybutyrate, carnitine and L-lactate in MCF-7 and MDA-MB-231 breast cancer cell lines, indicating that the effect was not specific to PANC-1 cells.

The ~50% reduction in intracellular L-lactate concentration and enhanced glycerol/glycine signal are consistent with the (*R,R'*)-MNF-associated attenuation of PKM2 levels and activity. Decreased PKM2 expression would result in an accumulation of phosphoenolpyruvate and its upstream precursor 2-phosphoglycerate. Since 2-phosphoglycerate is in equilibrium with 3-phosphoglycerate via the action of the reversible enzyme phosphoglycerate mutase, 3-phosphoglycerate concentrations will also increase. Indeed, the relationship between decreased PKM2 enzymatic activity and accumulation of 3-phosphoglycerate has been previously demonstrated.[32] In cancer cells, the glycolytic intermediate 3-phosphoglycerate enters the serine/glycine synthetic pathway to sustain anabolism[34] although serine metabolism rather than glycine appears to support nucleotide synthesis and tumor growth.[42] Thus, the enhanced glycerol/glycine signal observed in (*R,R'*)-MNF-treated PANC-1 cells is consistent with increased 3-phosphoglycerate levels due to defective PKM2. In addition, the accumulation of 3-phosphoglycerate may also produce changes in product-substrate equilibria for two upstream enzymes, phosphoglycerate kinase and glyceraldehyde phosphate dehydrogenase, resulting in increased levels of glyceraldehyde-3-phosphate. In turn, this metabolite is reversibly isomerized to the glycolytic intermediate, dihydroxyacetone phosphate, which is converted to glycerol-3-phosphate and dephosphorylated to glycerol by the recently identified mammalian glycerol-3-phosphate phosphatase (Figure 4B).[43] Thus, we surmise that the reduced intracellular concentrations of L-lactate and increased signals associated with glycerol/glycine following incubation with (*R,R'*)-MNF represent a significant disruption of the glycolytic process within PANC-1 cells. However, the possibility exists that the (*R,R'*)-MNF-induced increase in the glycerol/glycine signal may also originate from alterations in glycerophospholipid metabolism, one of the pathways identified in the metabolic pathway analysis of the metabolomics data, or by the increased biosynthesis of carnitine, as discussed below.

At the end of the PANC-1 xenograft arm of the study, the plasma concentrations of L-lactate were ~40% lower in animals receiving (*R,R'*)-MNF than control mice, consistent with an

attenuation of glycolysis similar to that observed in PANC-1 cells in culture. Decreased expression of PKM2 and HK2 in tumor tissues of (*R,R'*)-MNF-treated animals also supports this assumption. However, the intra-tumoral concentrations of L-lactate were ~30% greater in (*R,R'*)-MNF-treated animals compared to vehicle-treated mice. One explanation for this difference is the depletion in MCT4 transporter that was observed in tumor tissues after 21 days of exposure to (*R,R'*)-MNF but not in cell extracts after a 24h incubation. MCT4 is a member of the monocarboxylate transporter family encoded by the *SLC16A* family of genes and is the primary L-lactate exporter in glycolytic cancer cells.[44–46] Increased MCT4 expression is associated with a poor prognosis in pancreatic cancer[47] and inhibition of MCT4 expression and activity decreases pancreatic cell growth and viability and limits tumor growth.[44,47,48] Since the MCT4-encoded gene *SLC16A3* is activated by HIF-1α,[45,48] the (*R,R'*)-MNF-mediated decrease in MCT4 expression is consistent with the attenuation in the expression and nuclear translocation of HIF-1α in PANC-1 cells produced by GPR55 antagonists, including (*R,R'*)-MNF.[13]

Compared to plasma L-lactate levels, those found in tumor tissues were significantly elevated by ~12-fold and ~5-fold in (*R,R'*)-MNF-treated and control mice, respectively. Another member of the monocarboxylate transporter family, MCT1, mediates the intracellular import of L-lactate.[45] Since MCT1 expression is neither affected by HIF-1α nor upregulated in glycolytic tumors,[45] it is unlikely that treatment with (*R,R'*)-MNF would decrease MCT1 expression and/or function. Thus, it appears that both the relative rate of glycolysis and L-lactate export are negatively affected by (*R,R'*)-MNF treatment while L-lactate import remains relatively unchanged.

In addition to L-lactate export, MCT4 also plays a role in the cellular export of ketone bodies (e.g. β-hydroxybutyrate) while their import is mediated by MCT1.[45] Thus, the significant accumulation of β-hydroxybutyrate in serum-cultured PANC-1, MCF-7, and MDA-MB-231 cells may also reflect an (*R,R'*)-MNF-associated decrease in MCT4 expression without a significant effect on MCT1 expression and/or activity. Consistent with the cell-based studies and immunoblotting data of tumor tissues that showed significant reduction in MCT4 levels, (*R,R'*)-MNF-treated mice exhibited a significant increase (~180%) in plasma and intratumoral concentrations of β-hydroxybutyrate relative to control animals. For both groups of mice, the accumulation of β-hydroxybutyrate in tumor tissues was greater than in plasma, which concur with previously reported data in mice bearing a S2–013-derived pancreatic tumor[39] and the observation that ketone bodies are not metabolized in the human-derived Capan1 pancreatic cancer cell line.[39]

Incubation with (*R,R'*)-MNF also resulted in intracellular accumulation of carnitine in PANC-1, MCF-7, and MDA-MB-231 cells. Carnitine is generated from *ε-N*-trimethyllysine that is released from lysosomal or proteasomal degradation of proteins containing trimethyllysine residues.[49] Posttranslationally modified histones, such as H3K4me3, are potential sources of *ε-N*-trimethyllysine. Activation of the PI3K/AKT signaling pathway has been associated with increased H3K4me3 marks in breast cancer tumors and cell lines, and correlates with poor clinical outcome in breast, kidney, and colon cancers.[50] In addition, pSer37-PKM2 directly binds to histone H3 and phosphorylates it at threonine 11, which is required for histone H3 acetylation at lysine 9 and the subsequent expression of cyclin D1

and cMyc, cell proliferation, and tumorigenesis.[51] We have previously demonstrated that GPR55 inhibitors reduce PI3K/AKT signaling, impair nuclear translocation of pSer37-PKM2, and attenuate the expression of cyclin D1.[13] Here, we observed a decrease in PKM2 levels in PANC-1 tumor tissues of (*R,R'*)-MNF-treated mice. One can hypothesize that (*R,R'*)-MNF increases the existing pool of *ε-N*-trimethyllysine-containing histones for proteolysis, thereby increasing the amount of *ε-N*-trimethyllysine available for carnitine biosynthesis. The increase in carnitine biosynthesis is consistent with the enhanced glycerol/glycine signal observed in the (*R,R'*)-MNF-treated PANC-1 cells as glycine is formed during this process (Figure 4B).

The data from this study demonstrate that incubation of PANC-1 cells with (*R,R'*)-MNF attenuates the expression of the facilitative glucose and fructose transporter protein known as GLUT8 (*SLC2A8*). This intracellular hexose transporter is primarily localized to endoplasmic reticulum and lysosomes, although translocation to cellular membranes has been observed.[52–54] Increased expression of GLUT8 in endometrial adenocarcinoma relative to healthy tissue has been associated with tumor progression.[52] To our knowledge, our study is the first one that identified GLUT8 in a pancreatic cancer cell line and observed a treatment-associated decrease in its expression. Earlier studies have suggested a connection between AKT signaling and expression of *Slc2a* transcripts encoding facilitative transporter proteins.[52,54] Whether the (*R,R'*)-MNF-mediated attenuation of the PI3K-AKT signaling pathway accounts for the downregulation of GLUT8 will be examined in future studies. A novel glucose metabolism involving a hexose-6-phosphate dehydrogenase located within the endoplasmic reticulum has recently been identified in multiple cancer cell lines.[55] Since GLUT8 is localized to the endoplasmic reticulum, it may play a role in this process through active hexose transport. The impact of GPR55 inhibition —with (*R,R'*)-MNF or other molecules— in this process and on overall metabolic reprogramming through decreased GLUT8 protein expression will be reported elsewhere.

Previous studies in mice bearing tumors derived from C6 glioblastoma cells[29] and from U87MG glioblastoma cells[9] demonstrated that the administration of (*R,R'*)-MNF produces a significant reduction in tumor growth and that the data obtained in *in vitro* studies predicted *in vivo* activity. Thus, the failure of the current tumor xenograft study to affect PANC-1 tumor growth was unexpected. One potential explanation for this result is suggested by our recent studies of the anti-tumor activity of (R,R')-MNF in C6 glioblastoma cells, which express functional GPR55 and β2-AR.[9] The data from the study indicate that the bitopic effects of (R,R')-MNF—GPR55 inhibition and β2-AR activation-—work concurrently to disrupt pro-oncogenic signaling. Previous studies with PANC-1 cells have demonstrated that in these cells, β2-AR activation results in increased cellular growth.[58] Thus, the β2-AR agonist properties of (R,R')-MNF may cancel the compound's anti-tumor effects associated with GPR55. We have tested this hypothesis using the bitopic (R,S')-MNF, a diastereoisomer of (R,R')-MNF that has different β-AR selectivity and signaling.[13,59,60] The administration of (R,S')-MNF to mice bearing a PANC-1 xenograft produced a >70% inhibition in tumor growth (data not shown). The data from the (R,S')-MNF study will be reported elsewhere.

While the lack of an inhibitory effect on tumor growth was disappointing, the analysis of the plasma and tumor tissue samples indicated that the administration of (*R,R'*)-MNF led to reduced glycolysis in the PANC-1 tumor. Since β2-AR activation and GPR55 receptor inhibition may produce antagonistic effects on PANC-1 tumor growth, we used the C6 model to shed some light on the relative effect of these activities on glycolysis. The data demonstrate that incubation of C6 cells with (*R,R'*)-MNF decreased glucose consumption with a concomitant reduction in L-lactate release in the incubation media, indicating lower intracellular consumption of glucose and conversion to L-lactate. The data from the C6 studies also support a key role for the GPR55 antagonistic properties of (*R,R'*)-MNF towards glycolysis.

Two of the key observations from this study, the decreased expression of MCT4 and concomitant accumulation of L-lactate in tumor tissues of (*R,R'*)-MNF-treated animals, suggest a new research direction for (*R,R'*)-MNF and other GPR55 inhibitors. High levels of L-lactate have been correlated with tumor aggressiveness and poor prognosis[45] and increase in intracellular accumulation of L-lactate via MCT4 inhibition is associated with cytosolic acidification, inhibition of glycolysis, and cell death.[44,47] In addition, MCT4 is a key component of the “intercellular lactate shuttle” between glycolytic and oxidative cancer cells and in the crosstalk between cancer and endothelial and stromal cells.[45] Thus, the indirect inactivation of MCT4 by GPR55 inhibitors may be a new approach to the attenuation of these pathways that play a central role in tumorigenesis, growth, and metastasis. It is noteworthy that MCT4-mediated export of L-lactate into the tumor microenvironment plays a role in immunosuppression[45,48,56,57] and contributes to the poor response observed in pancreatic cancer immunotherapy.[56,57] The pre- and co-administration of (*R,R'*)-MNF may increase the effectiveness of immunotherapy and this possibility is currently under investigation.

Supplementary Material

Refer to Web version on PubMed Central for supplementary material.

Acknowledgments

The authors acknowledge the work and support of our colleagues from Crown Biosciences Inc., Beijing, China, who performed the PANC-1 tumor xenograft studies under contract from Mitchell Woods Pharmaceuticals, Inc. This work was supported by funds from the Intramural Research Program of the National Institute on Aging at NIH, from the National Institutes of Health (P30 GM103335) and the Nebraska Center for Integrated Biomolecular Communication Systems Biology Core (NIH National Institutes of General Medical Sciences P20-GM113126). The research was performed in facilities renovated with support from the National Institutes of Health (RR015468–01). This paper is subject to the NIH Public Access Policy.

Abbreviations used:

GLUT	facilitative glucose transporters
HK2	hexokinase 2
PKM2	pyruvate kinase M2
HIF	hypoxia-inducible factor

PDK1	phosphoinositide-dependent protein kinase-1
(*R,R'*)-MNF	(*R,R'*)-4'-methoxy-1-naphthylfenoterol
β_2-AR	β_2-adrenergic receptor
LC/MS	liquid chromatography-mass spectrometry
MCT	monocarboxylate transporter family

References

1. Warburg O. On the origin of cancer cells Science. 1956; 23:309–14.
2. Pelicano H, Martin DS, Xu RH, Huang P. Glycolysis inhibition for anticancer treatment Oncogene. 2006; 25:4633–46. [PubMed: 16892078]
3. Ganapathy-Kanniappan S, Geschwind JF. Tumor glycolysis as a target for cancer therapy: progress and prospects Mol Cancer. 2013; 12:152. [PubMed: 24298908]
4. Hamanaka RB, Chandel NS. Targeting glucose metabolism for cancer therapy J Exp Med. 2012; 209:211–5. [PubMed: 22330683]
5. Wu W, Zhao S. Metabolic changes in cancer: beyond the Warburg effect Acta Biochem Biophys Sin. 2013; 45:18–26.
6. Golding JP, Wardhaugh T, Patrick L, Turner M, Phillips JB, Bruce JI, Kimani SG. Targeting tumour energy metabolism potentiates the cytotoxicity of 5-aminolevulinic acid photodynamic therapy Br J Cancer. 2013; 109:976–82. [PubMed: 23860536]
7. Loar P, Wahl H, Kshirsagar M, Gossner G, Griffith K, Liu JR. Inhibition of glycolysis enhances cisplatin-induced apoptosis in ovarian cancer cells Am J Obstet Gynecol. 2010; 202:371.e1–8. [PubMed: 20138251]
8. Cheng G, Zielonka J, McAllister D, Tsai S, Dwinell MB, Kalyanaraman B. Profiling and targeting of cellular bioenergetics: inhibition of pancreatic cancer cell proliferation Br J Cancer. 2014; 111:85–93. [PubMed: 24867695]
9. Wnorowski A, Such J, Paul RK, Wersto RP, Indig FE, Jozwiak K, Bernier M, Wainer IW. Concurrent activation of β2-adrenergic receptor and blockage of GPR55 disrupts pro-oncogenic signaling in glioma cells Cell Signal. 2017; 36:176–88. [PubMed: 28495590]
10. Andradas C, Caffarel MM, Pérez-Gómez E, Salazar M, Lorente M, Velasco G, Guzmán M, Sánchez C. The orphan G protein-coupled receptor GPR55 promotes cancer cell proliferation via ERK Oncogene. 2011; 30:245–52. [PubMed: 20818416]
11. Ford LA, Roelofs AJ, Anavi-Goffer S, Mowat L, Simpson DG, Irving AJ, Rogers MJ, Rajnicek AM, Ross RA. A role for L-α-lysophosphatidylinositol and GPR55 in the modulation of migration, orientation and polarization of human breast cancer cells Br J Pharmacol. 2010; 160:762–71. [PubMed: 20590578]
12. Piñeiro R, Maffucci T, Falasca M. The putative cannabinoid receptor GPR55 defines a novel autocrine loop in cancer cell proliferation Oncogene. 2011; 30:142–52. [PubMed: 20838378]
13. Singh NS, Bernier M, Wainer IW. Selective GPR55 antagonism reduces chemoresistance in cancer cells Pharmacol Res. 2016; 111:757–66. [PubMed: 27423937]
14. Jozwiak K, Khalid C, Tanga MJ, Berzetei-Gurske I, Jimenez L, Kozocas JA, Woo A, Zhu W, Xiao R- P, Abernethy DR, Wainer IW. Comparative molecular field analysis of the binding of the stereoisomers of fenoterol and fenoterol derivatives to the β2-adrenergic receptor J Med Chem. 2007; 50:2903–15. [PubMed: 17506540]
15. Halouska S, Zhang B, Gaupp R, Lei S, Snell E, Fenton RJ, Barletta RG, Somerville GA, Powers R. Revisiting protocols for the NMR analysis of bacterial metabolomes J Integr OMICS. 2013; 3:120–37. [PubMed: 26078915]
16. Zhang B, Halouska S, Schiaffo CE, Sadykov MR, Somerville GA, Powers R. NMR analysis of a stress response metabolic signaling network J Proteome Res. 2011; 10:3743–54. [PubMed: 21692534]

17. Nguyen BD, Meng X, Donovan KJ, Shaka AJ. SOGGY: solvent-optimized double gradient spectroscopy for water suppression. A comparison with some existing techniques J Magn Reson. 2007; 184:263–74. [PubMed: 17126049]
18. Worley B, Powers R. MVAPACK: A Complete Data Handling Package for NMR Metabolomics ACS Chem Biol. 2014; 9:1138–44. [PubMed: 24576144]
19. Worley B, Powers R. Simultaneous phase and scatter correction for NMR datasets Chemometr Intell Lab Syst. 2014; 131:1–6. [PubMed: 24489421]
20. De Meyer T, Sinnaeve D, Van Gasse B, Tsiporkova E, Rietzschel ER, De Buyzere ML, Gillebert TC, Bekaert S, Martins JC, Van Criekinge W. NMR-Based characterization of metabolic alterations in hypertension using an adaptive, intelligent binning algorithm Anal Chem. 2008; 80:3783–90. [PubMed: 18419139]
21. Savorani F, Tomasi G, Engelsen SB. icoshift: A versatile tool for the rapid alignment of 1D NMR spectra J Magn Reson. 2010; 202:190–202. [PubMed: 20004603]
22. Xia J, Wishart DS. MetPA: a web-based metabolomics tool for pathway analysis and visualization Bioinformatics. 2010; 26:2342–4. [PubMed: 20628077]
23. Eriksson L, Trygg J, Wold S. CV-ANOVA for significance testing of PLS and OPLS models J Chemom. 2008; 22:594–600.
24. Shao J. Linear model selection by cross-validation J Am Stat Assoc. 1993; 88:486–94.
25. Xu QS, Liang YZ, Du YP. Monte Carlo cross-validation for selecting a model and estimating the prediction error in multivariate calibration J Chemom. 2004; 18:112–20.
26. Worley B, Halouska S, Powers R. Utilities for quantifying separation in PCA/PLS-DA scores plots Anal Biochem. 2013; 433:102–4. [PubMed: 23079505]
27. Benjamini Y, Hochberg Y. Controlling the false discovery rate: A practical and powerful approach to multiple testing J Roy Statist Soc Ser B. 1995; 57:289–300.
28. Worley B, Powers R. Multivariate analysis in metabolomics Curr Metabolomics. 2013; 1:92–107. [PubMed: 26078916]
29. Bernier M, Paul RK, Dossou KS, Wnorowski A, Ramamoorthy A, Paris A, Moaddel R, Cloix JF, Wainer IW. Antitumor activity of (R,R')-4-methoxy-1-naphthylfenoterol in a rat C6 glioma xenograft model in the mouse Pharmacol Res Perspect. 2013; 1:e00010. [PubMed: 25505565]
30. Yang W, Zheng Y, Xia Y, Ji H, Chen X, Guo F, Lyssiotis CA, Aldape K, Cantley LC, Lu Z. ERK1/2-dependent phosphorylation and nuclear translocation of PKM2 promotes the Warburg effect Nature Cell Biol. 2012; 14:1295–304. [PubMed: 23178880]
31. Ward PS, Thompson CB. Metabolic reprogramming: a cancer hallmark even warburg did not anticipate Cancer Cell. 2012; 21:297–308. [PubMed: 22439925]
32. Wong N, Ojo D, Yan J, Tang D. PKM2 contributes to cancer metabolism Cancer Lett. 2015; 356:184–91. [PubMed: 24508027]
33. Hofler A, Nichols T, Grant S, Lingardo L, Esposito EA, Gridley S, Murphy ST, Kath JC, Cronin CN, Kraus M, Alton G, Xie Z, Sutton S, Gehring M, Ermolieff J. Study of the PDK1/AKT signaling pathway using selective PDK1 inhibitors, HCS, and enhanced biochemical assays Anal Biochem. 2011; 414:179–86. [PubMed: 21402045]
34. Mathupala SP, Ko YH, Pedersen PL. Hexokinase II: cancer's double-edged sword acting as both facilitator and gatekeeper of malignancy when bound to mitochondria Oncogene. 2006; 25:4777–86. [PubMed: 16892090]
35. Bhardwaj V, Rizvi N, Lai MB, Lai JC, Bhushan A. Glycolytic enzyme inhibitors affect pancreatic cancer survival by modulating its signaling and energetics Anticancer Res. 2010; 30:743–9. [PubMed: 20392992]
36. Zhuo B, Li Y, Li Z, Qin H, Sun Q, Zhang F, Shen Y, Shi Y, Wang R. PI3K/Akt signaling mediated hexokinase-2 expression inhibits cell apoptosis and promotes tumor growth in pediatric osteosarcoma Biochem Biophys Res Commun. 2015; 464:401–6. [PubMed: 26116768]
37. Ogawa H, Nagano H, Konno M, Eguchi H, Koseki J, Kawamoto K, Nishida N, Colvin H, Tomokuni A, Tomimaru Y, Hama N, Wada H, Marubashi S, Kobayashi S, Mori M, Doki Y, Ishii H. The combination of expression of hexokinase 2 and pyruvate kinase M2 is a prognostic marker in patients with pancratic cancer Molec Clin Oncol. 2015; 3:563–71. [PubMed: 26137268]

38. Kaddurah-Daouk R, Krishnan KRR. Metabolomics: a global biochemical approach to the study of central nervous system diseases Neuropsychopharmacology. 2009; 34:173–86. [PubMed: 18843269]
39. Shukla SK, Gebregiorgis T, Purohit V, Chaika NV, Gunda V, Radhakrishnan P, Mehla K, Pipinos II, Powers R, Yu F, Singh PK. Metabolic reprogramming induced by ketone bodies diminishes pancreatic cancer cachexia Cancer Metab. 2014; 2:18. [PubMed: 25228990]
40. Navarrete A, Armitage EG, Musteanu M, Garcia A, Mastrangelo A, Bujak R, López-Casas PP, Hidalgo M, Barbas C. Metabolomic evaluation of Mitomycin C and rapamycin in a personalized treatment of pancreatic cancer Pharma Res Per. 2014; 2:e00067.
41. Amelio I, Cutruzzolá F, Antonov A, Agostini M, Melino G. Serine and glycine metabolism in cancer Trends Biochem Sci. 2014; 39:191–8. [PubMed: 24657017]
42. Labuschagne CF, van den Broek NJ, Mackay GM, Vousden KH, Maddocks OD. Serine, but not glycine, supports one-carbon metabolism and proliferation of cancer cells Cell Rep. 2014; 7:1248–58. [PubMed: 24813884]
43. Mugabo Y, Zhao S, Seifried A, Gezzar S, Al-Mass A, Zhang D, Lamontagne J, Attane C, Poursharifi P, Iglesias J, Joly E, Peyot ML, Gohla A, Madiraju SR, Prentki M. Identification of a mammalian glycerol-3-phosphate phosphatase: Role in metabolism and signaling in pancreatic β-cells and hepatocytes Proc Natl Acad Sci U S A. 2016; 113:E430–9. [PubMed: 26755581]
44. Draoui N, Feron O. Lactate shuttles at a glance: from physiological paradigms to anti-cancer treatments Dis Model Mech. 2011; 4:727–32. [PubMed: 22065843]
45. Pérez-Escuredo J, Dadhich RK, Dhup S, Cacace A, Van Hée VF, De Saedeleer CJ, Sboarina M, Rodriguez F, Fontenille MJ, Brisson L, Porporato PE, Sonveaux P. Lactate promotes glutamine uptake and metabolism in oxidative cancer cells Cell Cycle. 2016; 15:72–83. [PubMed: 26636483]
46. Andersen AP, Moreira JM, Pedersen SF. Interactions of ion transporters and channels with cancer cell metabolism and the tumor environment Phil Trans R Soc B. 2016; 369:20130098.
47. Baek G, Tse YF, Hu Z, Cox D, Buboltz N, McCue P, Yeo CJ, White MA, DeBerardinis RJ, Knudsen ES, Witkiewicz AK. MCT4 defines a glycolytic subtype of pancreatic cancer with poor prognosis and unique metabolic dependencies Cell Rep. 2014; 9:2233–49. [PubMed: 25497091]
48. Marchiq I, Pouyssegur J. Hypoxia, cancer metabolism and the therapeutic benefit of targeting lactate/H^+ symporters J Mol Med (Berl). 2016; 94:155–71. [PubMed: 26099350]
49. Servillo L, Giovane A, Cautela D, Castaldo D, Balestrieri ML. Where does N^{ϵ}-trimethyllysine for the carnitine biosynthesis in mammals come from? PLoS ONE. 2014; 9:e84589. [PubMed: 24454731]
50. Spangle JM, Dreijerink KM, Groner AC, Cheng H, Ohlson CE, Reyes J, Lin CY, Bradner J, Zhao JJ, Roberts TM, Brown M. PI3K/AKT signaling regulates H3K4 methylation in breast cancer Cell Rep. 2016; 15:2692–704. [PubMed: 27292631]
51. Yang W, Xia Y, Hawke D, Li X, Liang J, Xing D, Aldape K, Hunter T, Alfred Yung WK, Lu Z. PKM2 phosphorylates histone H3 and promotes gene transcription and tumorigenesis Cell. 2012; 150:685–96. [PubMed: 22901803]
52. Goldman NA, Katz EB, Glenn AS, Weldon RH, Jones JG, Lynch U, Fezzari MJ, Runowicz CD, Goldberg GL, Charron MJ. GLUT1 and GLUT8 in endometrium and endometrial adenocarcinoma Mod Pathol. 2006; 19:1429–36. [PubMed: 16892013]
53. Schmidt S, Joost H- G, Schürmann A. GLUT8, the enigmatic intracellular hexose transporter Am J Physiol Endocrinol Metab. 2009; 296:E614–8. [PubMed: 19176349]
54. Kim ST, Omurtag K, Moley KH. Decreased spermatogenesis, fertility and altered Slc2A expression in AKT1−/− and AKT2−/− testes and sperm Repro Sci. 2012; 19:31–42.
55. Marini C, Ravera S, Buschiazzo A, Bianchi G, Orengo AM, Bruno S, Bottoni G, Emionite L, Pastorino F, Monteverde E, Garaboldi L, Martella R, Salani B, Maggi D, Ponzoni M, Fais F, Raffaghello L, Sambuceti G. Discovery of a novel glucose metabolism in cancer: the role of endoplasmic reticulum beyond glycolysis and pentose phosphate shunt Sci Rep. 2016; 6:25092. [PubMed: 27121192]
56. Arcangeli A, Crociani O, Bencini L. Interaction of tumor cells with their microenvironment: ion channels and cell adhesion molecules. A focus on pancreatic cancer Phil Trans R Soc B. 2014; 369:20130101. [PubMed: 24493749]

57. Foley K, Kim V, Jaffee E, Zheng L. Current progress in immunotherapy for pancreatic cancer Cancer Lett. 2016; 381:244–51. [PubMed: 26723878]

58. Paul RK, Ramamoorthy A, Scheers J, Wersto RP, Toll L, Jimenez L, Bernier M, Wainer IW. Cannabinoid receptor activation correlates with the proapoptotic action of the β2-adrenergic agonist (R,R')-4-methoxy-1-naphthylfenoterol in HepG2 hepatocarcinoma cells J Pharmacol Exp Ther. 2012; 343:157–66. [PubMed: 22776956]

59. Woo AY- H, Jozwiak K, Toll L, Tanga MJ, Kozocas JA, Jimenez L, Huang Y, Song Y, Plazinska A, Pajak K, Paul RK, Bernier M, Wainer IW, Xiao R- P. Tyrosine 308 is necessary for ligand-directed Gs-biased signaling of β2-adrenoceptor J Biol Chem. 2014; 289:19351–63. [PubMed: 24831005]

60. Reinartz MT, Kälble S, Littmann T, Ozawa T, Dove S, Kaever V. Wainer IW, Seifert R. Structure-bias relationships for fenoterol stereoisomers in six molecular and cellular assays at the β2-adrenoceptor Naunyn Schmiedebergs Arch Pharmacol. 2015; 388:51–65. [PubMed: 25342094]

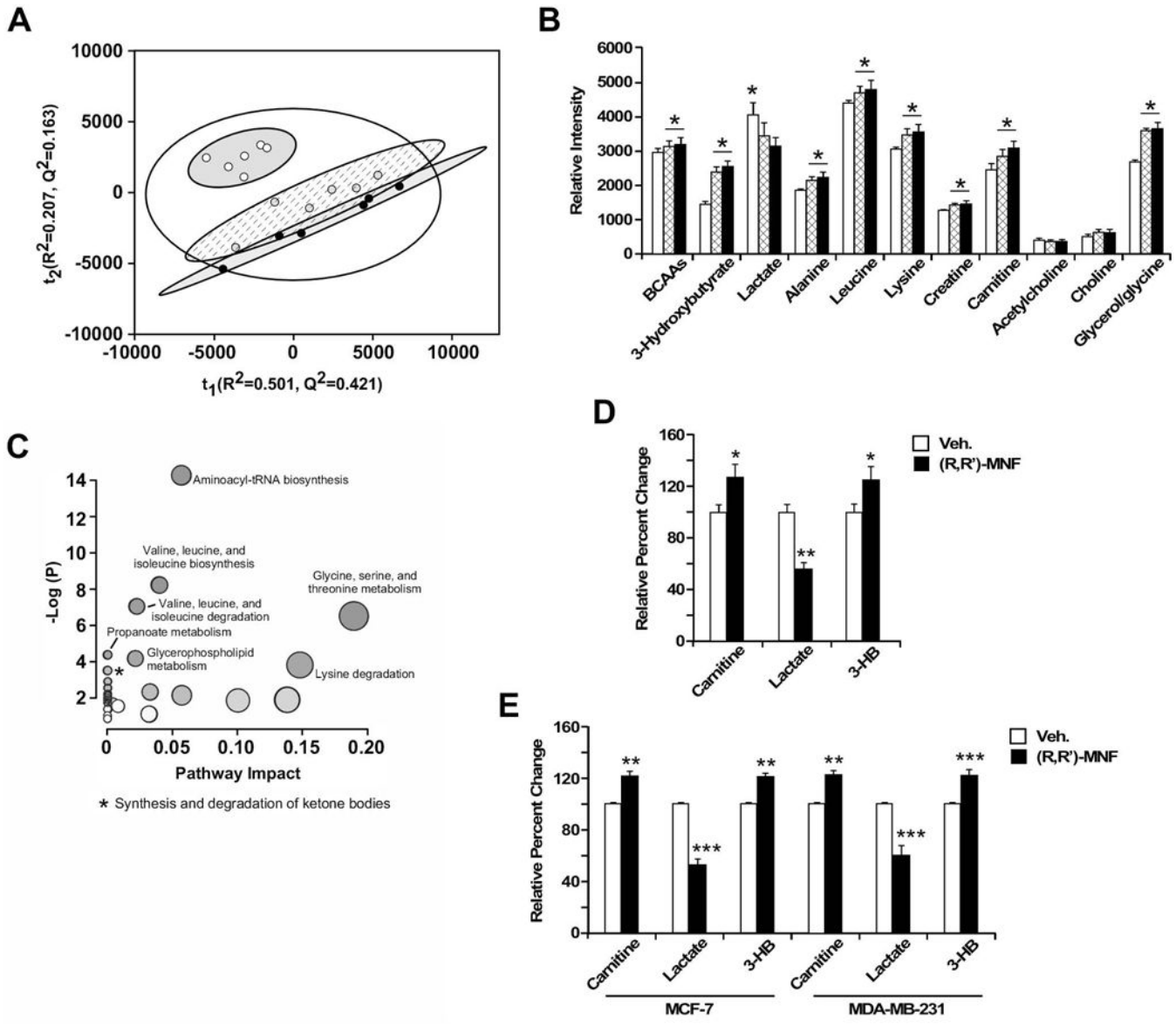

Figure 1. Metabolomics analysis on the effect of (*R,R'*)-MNF in PANC-1 cells.

(A) PCA scores resulting from modeling of the 1D ^{1}H NMR data matrix from untreated PANC-1 cells (open symbols) and PANC-1 cells treated with 0.5 μM (*R,R'*)-MNF (gray symbols) or 1 μM (*R,R'*)-MNF (black symbols). A statistically significant degree of separation is observed between treated and untreated groups. The ellipses correspond to 95% confidence intervals for a normal distribution. Each principal component is labeled with the corresponding R^2 and Q^2 values. (B) Bar graph of 1D ^{1}H NMR peak intensities (relative metabolite concentrations) resulting from the analysis of PANC-1 cellular extracts after a 1 h incubation with 0.5 μM (hatched bars) or 1 μM (filled bars) of (*R,R'*)-MNF versus untreated cells (open bars). Metabolites were identified from the back-scaled loadings plots as the major contributors to the group separations in the OPLS models (Figure S1A-D). Benjamini-Hochberg corrected student's *t* test *p*-values from pairwise comparisons are indicated. An asterisk indicates significance between the control and 1 μM of (*R,R'*)-MNF while an

asterisk with underlying bar indicates significance between the control and both treated groups. (C) Metabolic pathway analysis of the identified metabolites found in the 1D ^{1}H NMR spectra of the PANC-1 extracts after 1 h incubation with 0.5 μM or 1 μM of (*R,R'*)-MNF. Each circle represents a matched pathway and is colored according to its p-value from the pathway enrichment analysis. Statistically significant pathways ($P < 0.05$) are labeled with their common name. (D and E) Targeted metabolomics on the effect of 1 μM (*R,R'*)-MNF on intracellular concentrations of carnitine, L-lactate, and 3-hydroxybutyrate in PANC-1 cells (D) as well as MCF-7 and MDA-MD-321 breast tumor cells (E). *, $P \leq 0.05$; **, $P \leq 0.01$; *** $P \leq 0.001$.

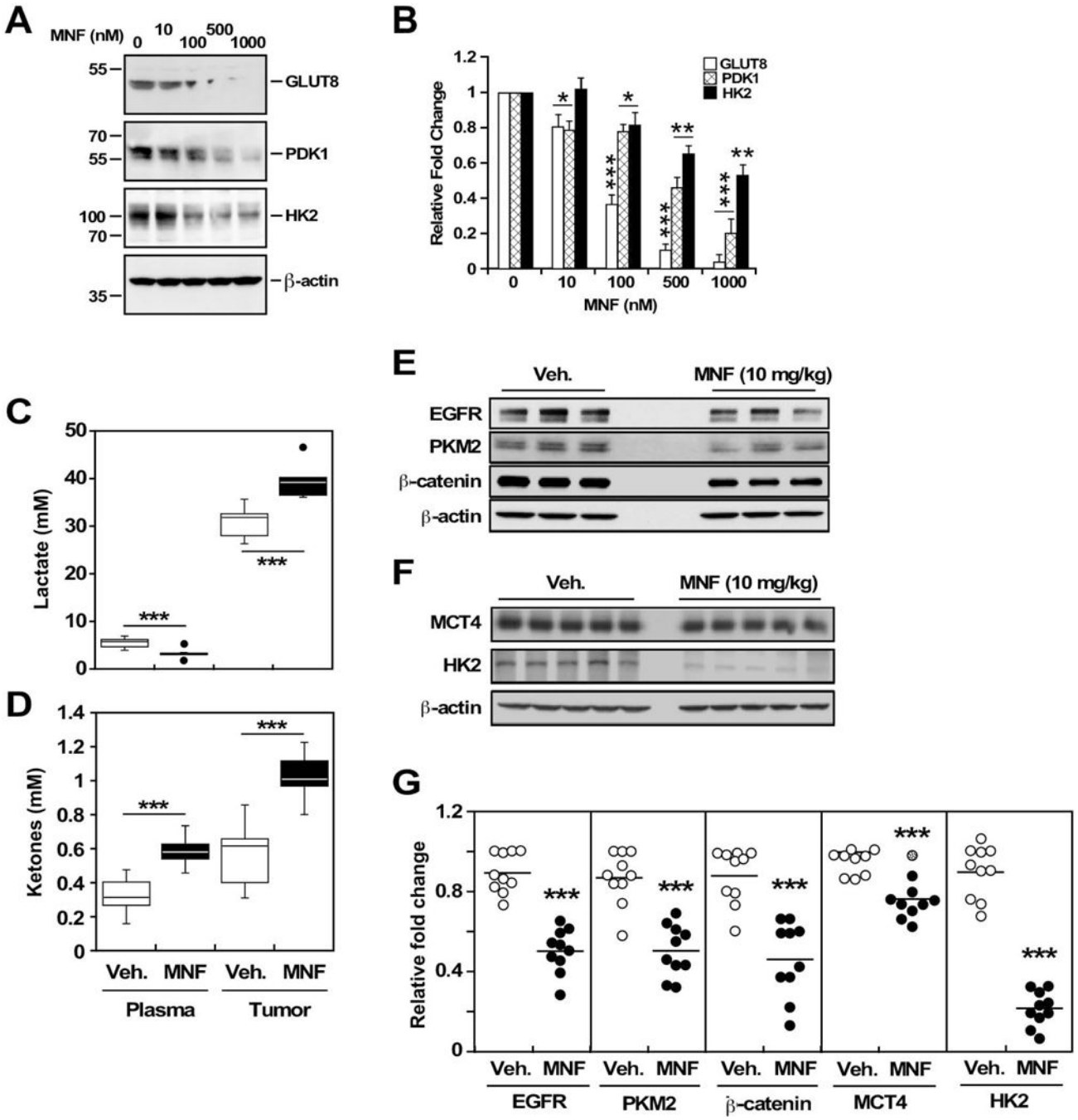

Figure 2. (*R,R'*)-MNF reduces expression of glycolytic regulators in PANC-1 cells and in PANC-1 xenograft tumors.

(A) PANC-1 cells were incubated with the indicated concentrations of (*R,R'*)-MNF (0–1 μM) for 24 h, after which cell lysates were prepared and immunoblotted with specific primary antibodies raised against GLUT8, PDK1, HK2, and β-actin, the latter serving as loading control. A representative experiment is depicted and full-length immunoblots are found in the Supplementary material. (B) Relative fold changes for GLUT8, PDK1, and HK2 were normalized to those of control cells and represented as bars ± SD (n=3 independent experiments). (C and D) Plasma and tumor concentration of L-lactate (C) and

ketone bodies (D) in a PANC-1 tumor xenograft model in nude mice after treatment with vehicle (Veh., n=10) or (*R,R'*)-MNF (10 $mg.kg^{-1}$, n=10) for 21 days. (E and F) PANC-1 tumor lysates were prepared and immunoblotted with the indicated primary antibodies, with β-actin serving as loading control. (G) Relative expression values for EGFR, PKM2, β-catenin, MCT4, and HK2 proteins in tumors excised from vehicle and (*R,R'*)-MNF-treated mice. *, $P \leq 0.05$; **, $P \leq 0.01$; *** $P \leq 0.001$.

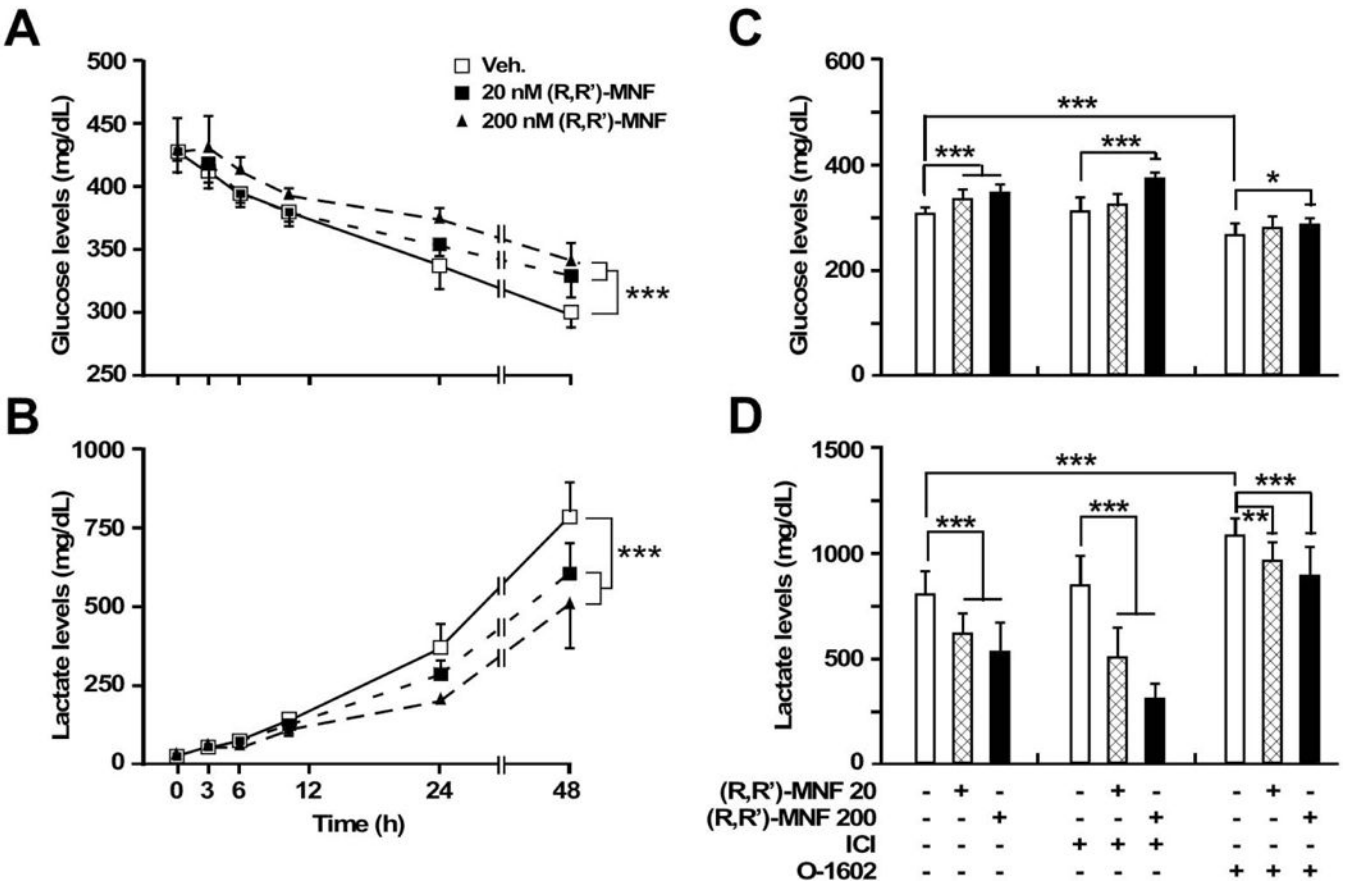

Figure 3. (*R,R'*)-MNF inhibits glucose uptake and lactate production in C6 glioma cells.

Serum-depleted rat C6 glioma cells were incubated with (*R,R'*)-MNF (0.02 and 0.2 μM) or vehicle (0.1% DMSO) for 48 h. At the indicated times, glucose (*panel A*) and lactate *(panel B*) levels were measured in the spent media. Effects of different concentrations of (*R,R'*)-MNF versus control were statistically evaluated at the 48 h time-point using one-way ANOVA and Tukey's post-hoc test. ***, $P < 0.001$. In a second series of experiments, C6 cells were pretreated with 100 nM of ICI 118,551 (selective β2-AR inhibitor) followed by the addition of MNF for 48 h. Moreover, (*R,R'*)-MNF-pretreated cells were incubated with 5 μM O-1602 (GPR55 activator) for 48 h. Glucose (*panel C*) and lactate (*panel D*) levels present in the spent media were measured. Bars represent mean ± SEM. Different letters denote statistically significant differences among treatments based on one-way ANOVA followed by Tukey's post-hoc test at $P \leq 0.05$.

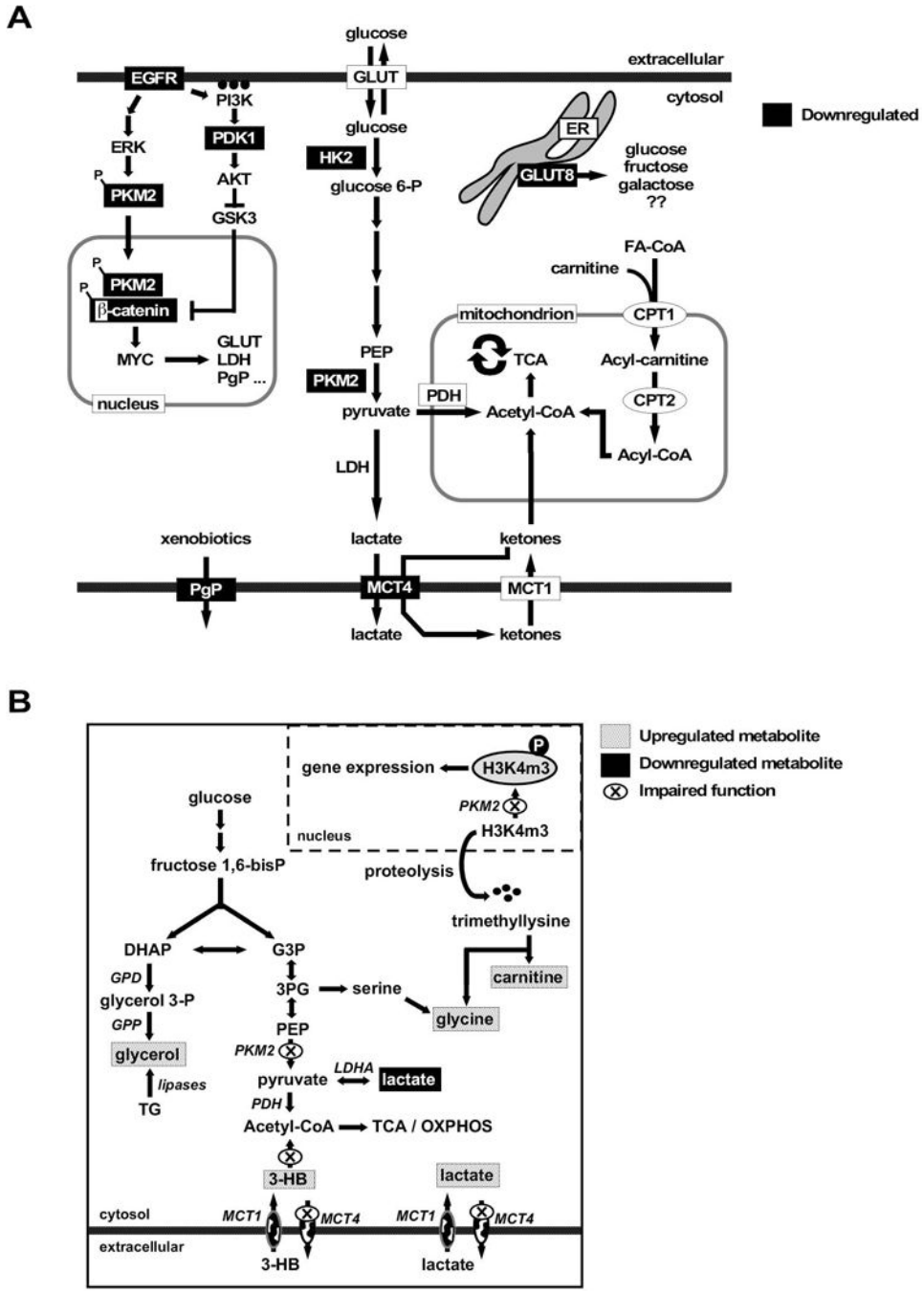

Figure 4.

(A) Schematic diagram of the signaling proteins involved in tumorigenesis that are inhibited by (*R,R'*)-MNF. (B) Global untargeted metabolomics analysis revealed a signature consistent with impairment in cancer glycolytic metabolism.